

***In vivo* photoacoustic imaging of tyrosinase expressing tumours in mice**

Jan Laufer*, Amit Jathoul†, Peter Johnson†+, Edward Zhang*,
Mark Lythgoe+, R Barbara Pedley†+, Martin Pule†+, Paul Beard*+
Department of Medical Physics & Bioengineering(*),
the Centre for Advanced Biomedical Imaging (+) and the UCL Cancer Institute (†),
University College London, London WC1E 6BT, UK

ABSTRACT

Two human tumour cell lines (K562, 293T) were stably transfected to achieve the genetic expression of tyrosinase, which is involved in the production of the pigment eumelanin. The cells were injected subcutaneously into nude mice to form tumour xenografts, which were imaged over a period of up to 26 days using an all-optical photoacoustic imaging system. 3D photoacoustic images of the tumours and the surrounding vasculature were acquired at excitation wavelengths ranging from 600nm to 770nm. The images showed tumour growth and continued tyrosinase expression over the full 26 day duration of the study. These findings were confirmed by histological analysis of excised tumour samples.

Keywords: Photoacoustic imaging, tomography, reporter gene, tyrosinase, Fabry-Perot polymer film ultrasound sensor, tumour, angiogenesis

1. INTRODUCTION

Reporter genes are widely used in preclinical research to study biological events such as gene expression, signalling pathways, cell proliferation and apoptosis. In photoacoustic imaging¹, genetically expressed fluorescent proteins have been used to implement the reporter gene concept in the relatively transparent zebrafish and *Drosophila* (fruitfly) pupa with image contrast being achieved by exciting at wavelengths that lie in the absorption band of the fluorophore². However, although some genetically expressed fluorescent proteins exhibit absorption into the red wavelength region³, relatively few provide strong absorption at near-infrared wavelengths where penetration depth in mammalian tissues is greatest. As a consequence their potential use in mouse models is restricted to superficial imaging applications. In addition, many fluorescent proteins lack photostability when illuminated by the high peak power laser pulses used in photoacoustic imaging. An alternative approach to creating optical absorption in otherwise translucent cells is the genetic expression of tyrosinase, an enzyme which is involved in the production of the endogenous pigment eumelanin. By transiently transfecting cells to express tyrosinase, it has been shown *in vitro*⁴ that eumelanin provides image contrast for photoacoustic imaging as well as magnetic resonance imaging. Using photoacoustic microscopy, it was also shown that tyrosinase expressing cells can be detected *in vivo*⁵ in the mouse ear. However, transient transfection also results in a significant drop in the expression of tyrosinase over a period of a few days⁵ therefore limiting the usefulness of this method for longitudinal studies.

In this study, mammalian tumour cells were stably transduced using an integrating retrovirus to genetically express the enzyme tyrosinase. The growth of subcutaneous tumours from these cells was visualised *in vivo* in mice in a longitudinal study using photoacoustic tomography. The suitability of this cell labelling approach for deep tissue imaging was also explored.

2. METHODS

Figure 1 shows a schematic of the photoacoustic imaging system. Low energy excitation pulses provided by a tunable OPO laser system were guided to the target using a multimode optical fibre. Following optical absorption in the tissue, the emitted photoacoustic waves were detected by a planar Fabry-Perot polymer film ultrasound sensor⁶. Its operation involves illuminating the sensor with the output of a wavelength-tuneable cw interrogation laser and detecting the intensity of the reflected light. By tuning the wavelength to the peak derivative of the interferometer transfer function, an acoustically induced modulation in the optical thickness of the interferometer produces a change in the reflected intensity

which is detected by a photodiode. By raster scanning the interrogation beam across the sensor, photoacoustic signals were acquired at multiple points from which 3D images were variously reconstructed using k-space⁷ or time reversal techniques⁸.

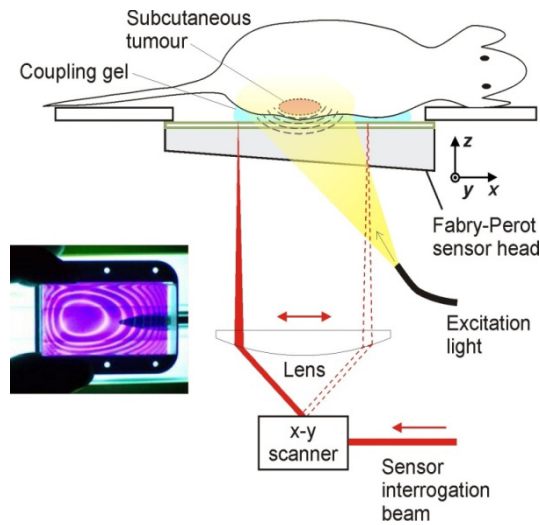


Figure 1 Schematic of the photoacoustic imaging system used to study subcutaneous, tyrosinase expressing tumours in nude mice. The photograph illustrates the transparency of the sensor, which allows backward mode imaging.

Integrating viral vectors were used to embed the vector transgene into the target cell genome so that cell and its progeny were permanently modified. The transgene contained the genetic information for the co-expression of not only tyrosinase but also CD34, a cell surface protein, to which a fluorescent marker was attached in order to sort the cells into a highly expressing population. Two cell lines (K562, 293T) were transduced. K562 are leukemia cells and 293T originated from embryonic human kidney cells. The tumours were grown subcutaneously in the flank of nude mice (MF1 nu/nu) by injecting a suspension of 5×10^6 cells in serum-free medium. The tumours were imaged several times over a period of up to 26 days using a photoacoustic scanner. The animals were anaesthetised using isoflurane and oxygen, and placed on the Fabry-Perot ultrasound sensor where an aqueous gel facilitated acoustic coupling. The beam diameter on the skin was 2cm, which resulted in a fluence of $<10 \text{mJ/cm}^2$ which is below the MPE for skin. Images were acquired at excitation wavelengths between 600nm and 770nm over a detection aperture of 14mm x 14mm with a step increment of 100 μm . The acquisition of a single image took 8min. Histological analysis was performed on formalin fixed slices of a 293T tumour. This involved staining the slices using haematoxylin and eosin (H&E) and Fontana Masson. H&E staining renders the cell nuclei as dark blue while eosin stains the cytoplasm a pink to red hue. Fontana Masson stains for eumelanin and produces a dark brown to black pigment.

3. RESULTS

Figure 2 shows x-y maximum intensity projections (MIP) of images of a 293T tumour and the surrounding vasculature acquired at different time points over a period of 26 days. The MIPs clearly show the growth of the tumour as indicated by the dashed circle, which provides a measure of the increase in the tumour diameter. Eumelanin was found to be a highly photostable compound. Extended periods of illumination with nanosecond laser pulses (around 1h per imaging session) on several separate imaging sessions did not produce evidence of photobleaching, which is often a feature of fluorescent proteins. Eumelanin provides strong photoacoustic contrast across the near-infrared wavelength region where tissue absorption is low, enabling penetration depths of several millimetres to be achieved. This is illustrated in Figure 3, which shows MIPs of another K563 tumour acquired at 600nm (Figure 3a), 680nm (Figure 3b), and 770nm (Figure 3c). The dashed circle in each image indicates the tumour location. Figure 3d shows the specific absorption coefficient spectra of oxy- and deoxyhaemoglobin, and eumelanin. It also shows the wavelength dependence of the optical penetration depth in soft tissue for a haemoglobin concentration of 2% and typical values of the scattering coefficient in skin and subdermis⁹. In Figure 3a ($\lambda=600\text{nm}$), the tumour is barely visible amongst the surrounding vasculature. By contrast, at the longer wavelengths the tumour can clearly be seen in Figure 3b and c. The difference in image contrast is

explained by the differences in the absorption exhibited by blood and eumelanin across the near-infrared spectrum (Figure 3d).

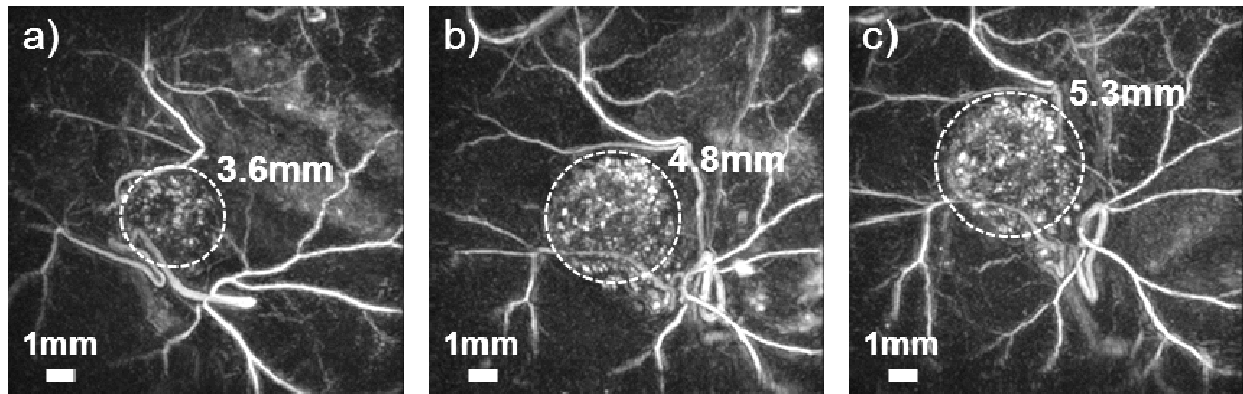


Figure 2 *x-y* maximum intensity projections of 3D photoacoustic images acquired on (a) day 7, (b) day 17, and (c) day 26 of a proliferating subcutaneous tumour formed of 293T cells ($\lambda=640\text{nm}$). The dashed circles around the tumour site provide an indication of the increase in tumour diameter. The cells were stably transduced to express tyrosinase, which leads to the production of eumelanin and provides the source of cellular contrast in the images.

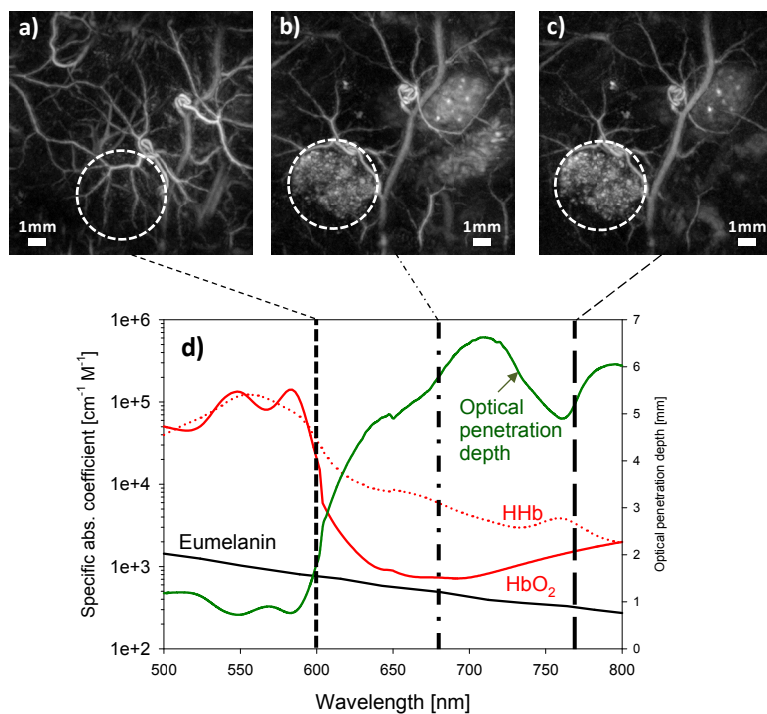


Figure 3 *x-y* MIPs of a subcutaneous tumour composed of tyrosinase-expressing K562 cells acquired at excitation wavelengths of (a) 600nm, (b) 680nm, and (c) 770nm. The location of the tumour is indicated by the dashed circle. (d) Specific absorption coefficient spectra of eumelanin, oxyhaemoglobin (HbO_2) and deoxyhaemoglobin (HHb), and the wavelength-dependent optical penetration depth. At 600nm, blood provides stronger optical absorption than the eumelanin produced by the cells, resulting in relatively low image contrast of the tumour. By contrast, at 680nm and 770nm the eumelanin in the tumour cells provide significantly stronger image contrast compared to blood.

The specific absorption coefficient of oxy- and deoxyhaemoglobin is more than one order of magnitude greater at 600nm than at 680nm and 770nm while the specific absorption of eumelanin only changes by 30% over the same wavelength

range. This means that blood provides far greater image contrast at 600nm compared to eumelanin, thus masking the relatively weak photoacoustic signal originating from the tumour cells. By contrast, the much lower absorption by blood at wavelengths longer than 680nm resulted in greater relative contrast of the tumour.

The demonstration of continued tyrosinase expression during tumour growth was a key aim of this study as it provides evidence of successful stable transduction of the cells with a transgene. As a consequence tyrosinase expression occurs in the daughter as well as the progenitor cells, enabling cell growth to be monitored. Histological analysis of excised 293T tumour samples showed abundant eumelanin within the tumour margins but not in other non-tumour tissue regions, such as the skin, the subcutaneous fat cell layer, or the connective tissue that surrounded the tumour. Figure 4 shows a section of the tumour core in which eumelanin staining using Fontana Masson resulted in a black pigment. This pigment could be found across the entire tumour but not in the surrounding tissue.

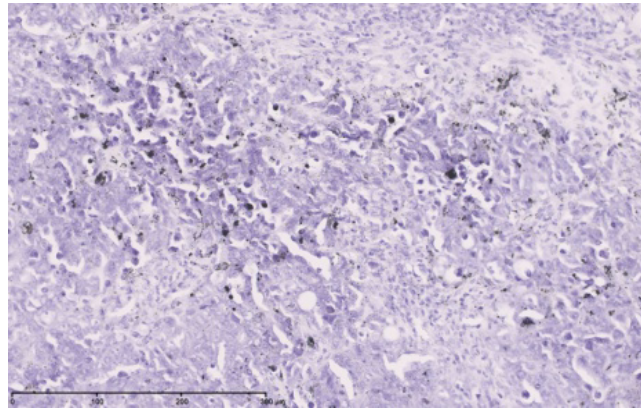


Figure 4 Light microscope image of a formalin fixed section of a 293T tumour stained with haematoxylin, eosin, and Fontana Masson. The presence of eumelanin is evident from the black marks, which represent eumelanin aggregations (melanosomes). The scale bar represents 300µm.

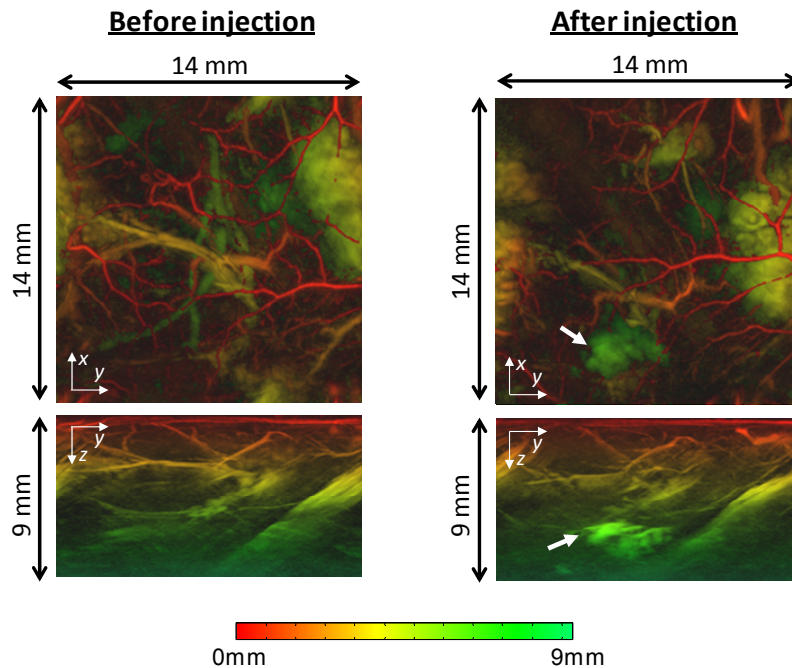


Figure 5 x - y and z - y MIPs (colour coded for depth) of the hind leg and abdomen of a nude mouse before and after the injection of tyrosinase expressing cells below the abdominal skin. The white arrows in the post-injection MIPs indicate the location of the cells at a depth of 6-8mm.

To provide an indication of the depth at which tyrosinase expressing cells could be detected, 1×10^6 K562 cells were injected subcutaneously in the lower abdomen of a nude mouse. This region was imaged before and immediately after the cell injection with the mouse lying on its side so that the leg was located between the sensor and the injected cells. MIPs (colour coded for depth) of these image data sets are shown in Figure 5. The pre-injection images show the superficial vasculature of the skin (red) as well as deeper blood vessels at 3-5mm depth (yellow and green). The large feature on the right hand side of the x - y MIPs is part of the abdominal wall. The cells are clearly visible at a depth of 6 to 8 mm in the post-injection MIPs.

4. CONCLUSIONS

Mammalian cells were stably transduced to express the enzyme tyrosinase, which resulted in the production of eumelanin. High resolution 3D photoacoustic images of subcutaneous tyrosinase expressing tumours were acquired in mice *in vivo*. The images showed tumour growth as well as the maintenance of strong tyrosinase expression during cell proliferation. The approach described in this study has a number of potential applications. Firstly, it extends the utility of photoacoustic imaging for studying tumour pathophysiology beyond visualising the vasculature alone, by providing a source of cellular contrast. The use of tyrosinase expressing cells should therefore enable researchers to follow both the early stage tumour cell proliferation and the concomitant formation of the vasculature, as well as the dynamic interplay between the two. In addition to this type of cell tracking application, modifying the transgene such that the expression of tyrosinase is activated by a specific promoter, photoacoustic imaging could be used to investigate a wide variety of cellular mechanisms in deep tissue in a non-invasive manner, such as the development of hypoxia with tumour growth as an indicator of potential therapeutic efficacy, or for tracking the response to therapy over time.

5. REFERENCES

- ¹ Beard, P., 2011. Biomedical photoacoustic imaging. *Interface Focus*, 1(4), pp.602-631.
- ² Razansky, D. et al., 2009. Multispectral opto-acoustic tomography of deep-seated fluorescent proteins in vivo. *Nature Photonics*, 3(June), pp.412-417.
- ³ Shaner NC, Campbell RE, Steinbach P, Giepmans BNG, Palmer AE, Tsien RY (2004) Improved monomeric red, orange and yellow fluorescent proteins derived from *Discosoma* sp. red fluorescent protein, *Nature Biotechnology*, 22(12), 1567.
- ⁴ Paproski R, Forbrich A, Wachowicz K, Hitt M, Zemp R, "Tyrosinase as a dual reporter gene for both photoacoustic and magnetic resonance imaging," *Biomed. Opt. Express*, 2, 771-780 (2011).
- ⁵ Krumholz A, Vanvickle-Chavez SJ, Yao J, Fleming TP, Gillanders WE, Wang LV (2011) Photoacoustic microscopy of tyrosinase reporter gene in vivo, *Journal of Biomedical Optics*, 16(8), 080503.
- ⁶ Zhang E, Laufer J, Beard P (2008) Backward-mode multiwavelength photoacoustic scanner using a planar Fabry-Perot polymer film ultrasound sensor for high-resolution three-dimensional imaging of biological tissues, *Applied Optics* 47, 561.
- ⁷ Köstli, KP, Beard, PC (2003) Two-dimensional photoacoustic imaging by use of Fourier-transform image reconstruction and a detector with an anisotropic response, *Applied Optics* 42(10), 1899-1908.
- ⁸ Treeby BE, Zhang EZ, Cox BT (2010) Photoacoustic tomography in absorbing acoustic media using time reversal, *Inverse Problems*, 26(11), 115003.
- ⁹ Simpson CR, Kohl M, Essenpreis M, Cope M (1998) Near infrared optical properties of ex-vivo human skin and subcutaneous tissues measured using the Monte Carlo inversion technique. *Physics in Medicine and Biology*, 43, 2465-2478.